Study on moisture loss and drying shrinkage behaviour of mortar with mineral admixture based on pore structure

S. Asamoto[1], T. Tsuji[1] and I. Kurashige[2]
[1]Department of Civil and Environmental engineering
Saitama University
255, Shi-Ohkubo, Sakura-ku, Saitama
JAPAN
[2]Central Research Institute of Electric Power Industry
1646 Abiko, Abiko-shi, Chiba
JAPAN
E-mail: asamoto@mail.saitama-u.ac.jp

Abstract: *The moisture loss and drying shrinkage behavior of mortar with mineral admixture such as blast-furnace slag and fly ash are investigated focusing on the microstructure affected by curing temperature. The curing at high temperature greatly accelerates the hydration reaction of the mortar with mineral admixture to make pore structure denser and leads to smaller moisture loss than that of mortar without mineral admixture. The moisture loss is almost proportional to the accumulated volume of pores whose radii are larger than the radius at the liquid/vapour interface based on the Kelvin equation and BET theory of absorbed water. When the shrinkage is assumed to be induced only by the capillary tension, the estimated shrinkage shows different tendency from experimental one. It suggests that the other shrinkage driving forces that have been believed to be dominant under severe drying conditions should be taken into account even under normal drying condition (RH=60% at 20 degree).*

Keywords: *Granulated blast-furnace slag, Fly ash, Shrinkage, Moisture loss, Curing temperature*

1. INTRODUCTION

Mineral admixtures such as blast-furnace slag and fly ash have been widely used replacing with cement in Japan in order to reduce CO_2 emission arising from the cement production. Since they retard the hydration reaction and decrease the hydration heat, the application is mainly to the massive concrete for dam or underground structures. It has been reported, however, that numerous shrinkage cracks were found in the massive concrete structures using the slag cement. Although the slow strength development, small tensile creep, large autogenous shrinkage and others due to the slag replacement are considered as the reasons for the cracking, it has been not consistently understood since they are strongly dependent on mix proportion, curing, and boundary conditions. In the case of the concrete containing fly ash, such serious problems have not yet been reported but it is important to comprehend the possibility of the shrinkage cracking consistently in order to avoid the unexpected damage in the structures.

The hydration reaction of the concrete with mineral admixtures is dependent on the curing temperature. The internal part of the massive concrete structure and the precast concrete with admixture that has been recently used are exposed to high temperature at early ages and the microstructure at elevated temperature could be changed. In this paper, the authors study the influence of curing temperature on moisture loss and drying shrinkage of mortar with blast-furnace slag and fly ash focusing on the microstructure.

2. EXPERIMENTAL PROGRAM

2.1. Materials

The mortar with or without mineral admixture was cast. The mix proportions are given in Table 1. Water-binder ratio is 50 % and the volume ratio of the fine aggregate is 40 % in all specimens. The specimen without mineral admixture is named OPC, while the specimens containing blast-furnace slag and fly ash are referred as BS30 and FA20, respectively. The weight replacement ratios of slag and fly ash with cement are 30% and 20%, respectively.

Table 1 Mix proportions of mortar (kg/m^3)

Specimen	Water to Binder ratio	Water	**Cement** Ordinary Portland cement Specific gravity: 3.15 Blaine specific surface: 3260cm^2/g	**Slag** BF4000 slag Specific gravity: 2.89 Blaine specific surface: 4440cm^2/g	**Fly ash** II type of fly ash Specific gravity: 2.24 Blaine specific surface: 4130cm^2/g	**Fine aggregate** River sand Specific gravity: 2.52
OPC	50 %	367	734	—	—	1028
BS30	50 %	363	509	218	—	1028
FA20	50 %	356	569	—	142	1028

2.2. Moisture Loss and Drying Shrinkage Test

Prismatic mortar specimens with 40 x 40 mm cross section and 160 mm length were used for the test. The form was removed one day after casting and then all specimens were adequately cured in water (submerged) at 20 or 60 ºC. At seven days of age, each specimen was dried at a relative humidity of 60% and 20 ºC in the controlled chamber. Although the water curing at 60 ºC is not probable in reality, the extreme condition was provided in order to clearly comprehend the phenomena and the mechanism which affect the moisture loss and drying shrinkage. During drying, moisture loss and shrinkage were simultaneously measured using the same specimen. Moisture loss was obtained by dividing the reduction of the specimen weight after the curing by the volume. Longitudinal length change at 100 mm center part on the surface of the specimen was measured with the contact gauge having 0.001 mm resolution. All of results were obtained by averaging values of three specimens.

2.2. Mercury Intrusion Porosimetry (MIP) Test

The mercury intrusion porosimetry (MIP) test was curried out to examine the pore structure of each specimen. The 56 days dried specimens used for moisture loss and shrinkage test were stored under sealing condition at 20 ºC for about 2 months and then crushed into small pieces from 4 mm to 5 mm. The small pieces were exposed to D-dry (vacuum drying at –80 ºC) for 120 hours to measure the pore structure with mercury intrusion porosimeter. The surface tension of mercury and the contact angle between mercury and sample are set to 0.484 N/m and 130°, respectively. Assuming that the pore structure is assumed to be cylinder, the volume of each pore size from 3.3 nm to 360 μm was measured and obtained averaging the two measured values.

3. EXPERIMENTAL RESULTS AND DISCUSSION

3.1. Moisture Loss

Firstly, the influence of the curing temperature on moisture loss at drying is discussed. Figures 1 and 2 represent the moisture loss of mortar exposed to the drying condition (RH=60% at 20 °C) after 7 days curing in water of 20 and 60 °C, respectively. The 20 °C curing condition provides the smallest moisture loss of OPC mortar, while the moisture loss of OPC specimen is the largest in the case of 60 °C curing. The slower hydration reaction of specimen with mineral admixture under normal temperature makes microstructure coarser after the curing at 20 °C and results in larger moisture loss of mortars with slag and fly ash than that of OPC specimen. On the other hand, the reaction of BS30 and FA20 specimens due to the latent hydraulic property of slag and pozzolanic reaction with $Ca(OH)_2$ is promoted during 7 days curing in 60 °C water and denser pore structure leads to retard of moisture evaporation from the specimens. When the fly ash is contained in the mortar, especially, the reaction at the elevated temperature could be significantly accelerated and results in the considerable reduction of the moisture loss comparing to that after 20 °C curing. It indicates that the temperature sensitivity of hydration reaction of fly ash cement is more significant than that of slag cement.

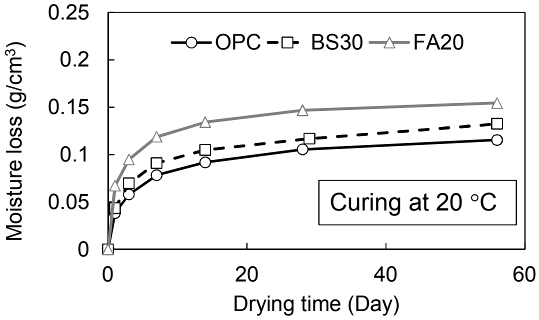

Figure 1 Moisture loss of each specimen (Curing at 20 °C)

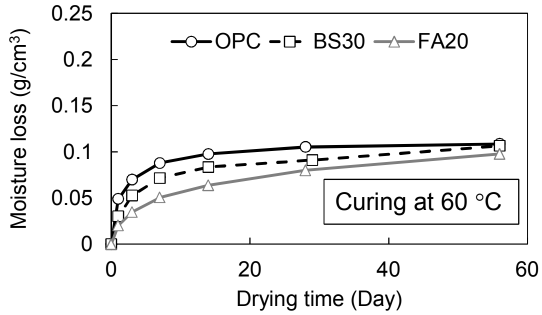

Figure 2 Moisture loss of each specimen (Curing at 60 °C)

Figures 3 and 4 show the pore size distribution obtained by MIP test. There is more volume of relatively large pores with more than 10 nm in mortars with slag and fly ash than that in OPC specimen. The curing at high temperature fills the relatively large pores with hydration products and increases the volume of fine pores with less than 10 nm size as shown in Figure 4. The fine pores are formed the most in the case of FA20 specimens. The result of the pore size distribution also indicates that the reaction of fly ash cement is the most sensitive to curing temperature and the promotion makes the pore structure dense.

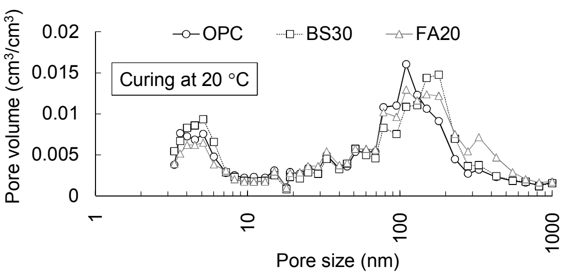

Figure 3 Pore size distribution of each specimen after drying (Curing at 20 °C)

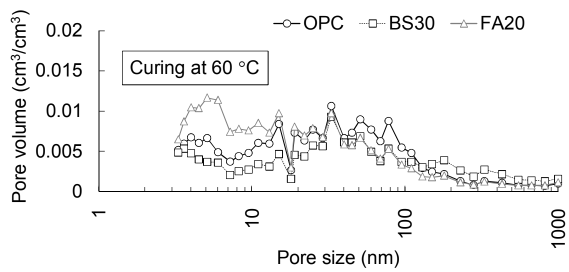

Figure 4 Pore size distribution of each specimen after drying (Curing at 60 °C)

Next, the moisture loss behavior under the drying of RH=60% at 20 °C is discussed based on the pore structure. According to Maekawa et al. (1999), the pore radius r_c, which is at the equilibrated interface between liquid and vapor, is identified as shown below.

$$r_c = Cr_s, where \;\; C = 2.15 \tag{1)}$$

$$r_s = \frac{2\gamma M_w}{\rho RT \ln h} \tag{2)}$$

where, γ: surface tension of water [N/m], ρ: density of liquid water [kg/m^3], R: the gas constant [J/mol/K], T: absolute temperature [K], M_w: molecular mass of the water [kg/m^3], and h: relative humidity, and the constant C has been obtained after numerous comparisons of the analytical predictions of the equilibrated interface radii, r_c, as obtained from the modified BET theory and r_s as given by Kelvin equation. Since the r_c under the drying condition (RH=60% at 20 °C) is calculated as about 4.5 nm according to Eq3. (1), the moisture existed in the pores larger than 9 nm could evaporate at equilibrium of the drying. Thus, the volume of pores larger than 9.5 nm obtained by the MIP test is accumulated and the results of all specimens are summarized as shown in Tables 2 and 3.

In the case of BS 30 and FA20 specimens, the accumulated volume of the pores larger than 9.5 nm is decreased when the water curing at 60 °C is provided, while the pores volume of OPC specimen is not so different in curing temperature. This result also suggests that the evaporable water which existed in the pores larger than 9.5 nm is reduced after curing at elevated temperature in the case of mortar with mineral admixture and results in the smaller moisture loss than that of mortar without admixture, as mentioned above.

The order of the accumulated volume of pores larger than 9.5 nm in each specimen cured at 20 °C is almost proportional to the order of moisture loss as shown in Figure 1. Although the pores volume larger than 9.5 nm in BS30 specimen is slightly smaller than that in OPC specimen with larger moisture loss, it could be attributed to the gradual pore structure formation of BS30 specimen during drying due to slower hydration reaction. The coarser pore structure of BS30 specimen at the beginning of drying after the curing could disperse more moisture than OPC specimen and lead to larger moisture loss even at 56 days of drying.

The accumulated volume of pores larger than 9.5 nm in BS30 specimen cured at 60 °C is much smaller than that of FA20 specimen but the moisture loss of BS30 specimen is larger than that of FA20 specimen. It could be ascribed to the moisture trapped in the inkbottle-shaped pores as shown in Figure 5. It is reported (Maekawa et al 1999) that the probability water entrapment in a pore of radius r larger than the pores of radius r_c would be dependent on the accumulated volume of the pores whose radius is smaller than r_c (This probability means to be dependent on the chance of intersection of the larger pores with the smaller completely filled pores). Table 2 indicates that the volume of fine pores whose radius is smaller than r_c in FA20 specimen is much more than that in BS30 specimen. Thus, such more fine pores of FA20 specimen trapped more moisture in the pores with the radius larger than r_c and leads to smaller moisture loss than that of BS30 specimen. It is concluded that the equilibrated moisture loss of each specimen with different mix proportions and curing temperature can be almost interpreted considering the accumulated volume of pores with radius larger or smaller than the equilibrated interface radius r_c.

Table 2 Accumulated volume of pores from 3.3 nm to 9.5nm and 9.5 nm to 360 μm (Curing at 20 °C)

Specimen	Pore size from 3.3 nm to 9.5nm (cm^3/cm^3)	Pore size from 9.5 nm to 360 μm (cm^3/cm^3)
OPC	0.0429	0.1654
BS30	0.0499	0.1647
FA20	0.0367	0.1841

Table 2 Accumulated volume of pores from 3.3 nm to 9.5nm and 9.5 nm to 360 μm (Curing at 60 °C)

Specimen	Pore size from 3.3 nm to 9.5nm (cm^3/cm^3)	Pore size from 9.5 nm to 360 μm (cm^3/cm^3)
OPC	0.0434	0.1673
BS30	0.0306	0.1419
FA20	0.0741	0.1548

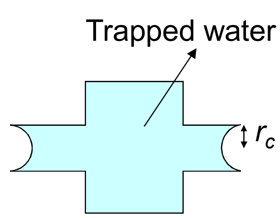

Figure 5 Trapped water in inkbottle-shaped pores

3.2. Drying Shrinkage

The results of drying shrinkage of each specimen are shown in Figures 6 and 7. The drying shrinkage is not so different in each specimen. Focusing on the curing temperature, when specimens are cured at 60ºC, the drying shrinkage is smaller than that of specimens that are cured at 20 °C in all cases. As mentioned above, the curing at elevated temperature can promote the hydration process and achieve fine pore structure. It is concluded that dense pore structure due to the progressive curing can cause larger elastic stiffness and smaller moisture loss and result in smaller shrinkage of specimens.

Here, the shrinkage behaviour of each specimen is discussed only focusing on the capillary tension theory (Powers, 1968) that has been believed to be the most dominant under normal drying condition (room temperature and moderate relative humidity). The capillary tension P_c at equilibrium is expressed using the parameters in Eq. (2) as below.

$$P_c = -\frac{2\gamma}{r_s} \tag{3}$$

The capillary force which acts in the pores is proportional to the surface area of pores where moisture exists. Thus, the shrinkage stress S_c arising from the capillary tension in saturated pores is idealized as,

$$S_c = P_c \frac{A_s}{A_t} = -\frac{2\gamma}{r_s}\frac{A_s}{A_t} \tag{4}$$

where, A_s is the surface area of pores where moisture exists at equilibrium and A_t is the total surface area of pores. Since the surface area of pores is dependent to the pores volume, in the paper, the surface area fraction A_s/A_t is assumed to simply be proportional to the pores volume fraction V_s/V_t (V_s: accumulated volume of pores larger than 9.5 nm(≈2 x r_c), V_t: total accumulated pores). Table 3 summarizes the V_s/V_t of each specimen.

Since P_c is the same at equilibrium in all cases, the shrinkage stress due to the capillary tension could be dependent on the V_s/V_t. The amount of the shrinkage at equilibrium also depends on the Young's modulus of the specimens. The Young's modulus after 56 days of drying was measured using ϕ50 x 100 mm cylinder specimens and the results are given in Figure 8. According to Table 3 and Figure 8, when curing temperature is 20 °C, BS30 with the largest V_s/V_t and relatively small Young's modulus should shrink the most but such tendency was not observed in reality. In the case of curing at 60 °C, the V_s/V_t of FA20 specimen is 1.5 times larger than that of other specimens and leads to about 1.5 times larger shrinkage based on the capillary theory, because the Young's modulus is not so different in each specimen. In the experiment, however, the shrinkage of FA20 specimen at equilibrium is slightly larger than that of other specimens. Consequently, it is difficult to explain the amount of shrinkage at equilibrium only from a viewpoint of capillary theory. Other shrinkage mechanisms such as disjoining pressure and surface energy of C-S-H gel (Powers, 1968) which have been believed to be dominant under severe drying condition should be taken into account for consistent discussion of shrinkage behavior depending on the mix proportion and curing temperature.

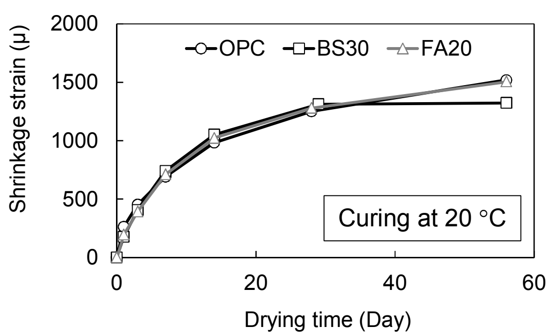

Figure 6 Drying shrinkage of each specimen (Curing at 20 °C)

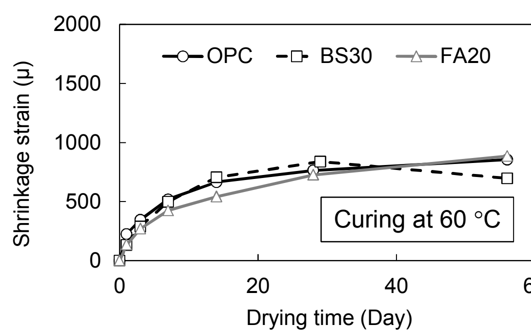

Figure 7 Drying shrinkage of each specimen (Curing at 60 °C)

Table 3 V_s/V_t of each specimen

Curing temperature	Specimen	V_s/V_t
20 °C	OPC	0.206
	BS30	0.233
	FA20	0.166
60 °C	OPC	0.206
	BS30	0.177
	FA20	0.324

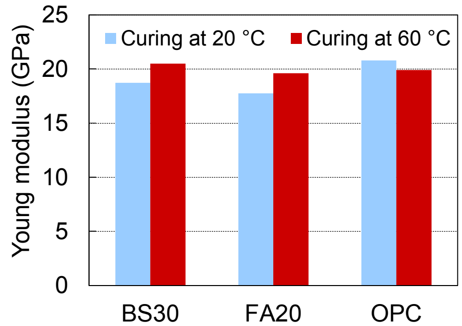

Figure 8 Young's modulus of each specimen after curing

4. CONCLUSION

In this paper, the moisture loss and drying shrinkage behavior of mortar with blast-furnace slag and fly ash are discussed from a viewpoint of the microstructure affected by curing temperature. Key findings are summarized below.

i) The curing at high temperature greatly accelerates the hydration reaction of the mortar with mineral admixture to make pore structure denser and leads to smaller moisture loss than that of mortar without mineral admixture.
ii) The equilibrated moisture loss of each specimen with different mix proportions and curing temperature can be almost estimated based on the accumulated volume of pores with radius larger or smaller than the equilibrated interface radius between liquid and vapor.
iii) When the shrinkage is assumed to be induced only by the capillary tension, the estimated shrinkage from the shrinkage force and Young's modulus shows different tendency among mix proportions from experimental one. It suggests that the other shrinkage driving forces that have been believed to be dominant under severe drying condition should be taken into account even under normal drying condition of RH=60% at 20 °C.

5. ACKNOWLEDGEMENT

This study is financially supported by JSPS Grant-in-Aid for Young Scientists (B) 21760342. The authors gratefully acknowledge the financial support.

6. REFERENCES

Maekawa, K., Chaube, R. and Kishi, T. (1999), *Modeling of Concrete Performance*, E & FN SPON, London, pp.59-106

Powers, T.C. (1968), *Mechanisms of shrinkage and reversible creep of hardened cement paste*, *Proceeding of International Conference on the Structure of Concrete*, Cement and Concrete Association, 1965, London, pp.319-344